



An Ecomorphological Approach to Craniomandibular Integration in Neotropical Deer

Guillermo H. Cassini^{1,2,3} · Néstor Toledo^{4,3}

Published online: 3 April 2020

© Springer Science+Business Media, LLC, part of Springer Nature 2020

Abstract

South American cervids have a relatively recent evolutionary history in the Neotropics. Present taxonomical richness includes six genera and 17 species grouped in at least two clades, Blastocerina and Odocoileina. With few exceptions, functional morphology or ecomorphological approaches have not been rigorously applied to the masticatory apparatus of Neotropical deer. In order to understand the relationship between craniomandibular integration and feeding behavior, we used geometric morphometric methods (3D landmarks) to quantify the strength and significance of the correlation between morphology and feeding behavior. Two blocks Partial Least Squares analyses, angular comparison, regression analysis, and independent contrast were performed to explore the patterns of covariation between cranial and mandibular shape and size, and between them and continuous dietary characters. The main variation in shape is related to a gradient from a brachycephalic cranium with a robust mandible in small deer to a dolicocephalic cranium with a gracile mandible in large deer. These shape changes seem to be modeled by a complex interplay of allometric trends and biomechanically significant features related to the proportions of dietary monocotyledon, fruit, or dicotyledonous plant material. We find remarkable convergences in the brocket deer ecomorphotype in the two clades of Neotropical cervids, as well as similar craniomandibular traits between marsh and pampas deer with African mixed feeder bovinds related to monocotyledon consumption. These findings lead us to share Radinsky's interest in convergences in the masticatory apparatus of herbivorous mammals.

Keywords Skull integration · Jaw biomechanics · Brocket ecomorphotype · Herbivorous morphofunctional convergences · 3D landmarks · Radinsky

Electronic supplementary material The online version of this article (<https://doi.org/10.1007/s10914-020-09499-5>) contains supplementary material, which is available to authorized users.

✉ Guillermo H. Cassini
gcassini@macn.gov.ar

- ¹ División Mastozoología, Museo Argentino de Ciencias Naturales “Bernardino Rivadavia”, Av. Ángel Gallardo 470, C1405DJR Ciudad Autónoma de Buenos Aires, Argentina
- ² Departamento de Ciencias Básicas, Universidad Nacional de Luján, Ruta 5 y Av. Constitución s/n, 6700 Luján, Buenos Aires, Argentina
- ³ Consejo Nacional de Investigaciones Científicas y Técnicas (CONICET), Ciudad Autónoma de Buenos Aires, Argentina
- ⁴ División Paleontología Vertebrados, Unidades de Investigación Anexo Museo, Museo de La Plata, Facultad de Ciencias Naturales y Museo, Av. 60 y 122, 1900 La Plata, Argentina

Introduction

Fifty years ago, the considerable parallelism in the early evolution of Perissodactyla drew Radinsky's (1969) attention. His interest in functional and adaptive explanations for the evolutionary changes was evident during the course of his professional career (Kay 2019). Radinsky (1985) was interested in how morphological variation correlates with phylogenetic relationships and ecology, and studied the biomechanics of the ungulate jaw apparatus. In chapter 17 of the posthumously published “The Evolution of Vertebrate Design,” Radinsky (1987) expressed intrigue in the convergences of the masticatory and locomotor apparatus of distant lineages of herbivorous mammals.

Today, terrestrial artiodactyls constitute the morphologically and taxonomically richest and most diverse clade of extant ungulates (Janis 2007). In South America they have become the most diverse small to large herbivores, represented mainly

by cervids (Cassini et al. 2016). The phylogenetic analyses of Duarte et al. (2008) highlighted convergent evolution for brocket deer morphology in Neotropical deer. This seems to occur at least once in both Blastocerina and Odocoileina sensu Heckeberg et al. (2016). Here, we honor Leonard Radinsky's work by studying these morphological convergences in an ecomorphological approach, using geometric morphometric methods to evaluate the morphological integration between the cranium and mandible of Neotropical deer.

Neotropical Deer

The evolutionary history of cervids in South America is relatively recent; they arrived approximately 1.8 Ma in the early Pleistocene and survive to Recent times (Cassini et al. 2016). According to current hypotheses Neotropical deer are united in Capreolinae (with *Alces*, *Capreolus*, *Hydropotes*, and *Rangifer*) and are represented by six genera: *Blastocerus* (marsh deer), *Hippocamelus* (huemuls), *Mazama* (brockets), *Odocoileus* (white-tailed deer), *Ozotoceros* (pampas deer), and *Pudu* (pudus) with 17 species recognized (Duarte and González 2010). Recent phylogenetic studies highlighted the paraphyly of *Hippocamelus* and *Pudu*, and the polyphyly of *Mazama* (see Gutiérrez et al. 2017 and references therein). With the exception of *Pudu mephistophiles*, Neotropical deer are included in Blastocerina (sensu Heckeberg et al. 2016), including *B. dichotomus*, *H. antisensis*, *H. bisulcus*, *M. chunyi*, *M. gouazoubira*, *M. nemorivaga*, *Ozotoceros bezoarticus*, and *Pudu puda*, and Odocoileina (sensu Heckeberg et al. 2016), including *M. americana*, *M. bororo*, *M. bricenii*, *M. nana*, *M. pandora*, *M. temama*, *M. rufina*, and *Odocoileus virginianus*. As is evident, recent deer richness is dominated by species of *Mazama*, the brockets, which are characterized by spike-like antlers.

Neotropical deer occupy a variety of environments, from lowland plains to high mountains, each with open or closed and dry or wet regions (Merino and Rossi 2010). In many cases the geographic distribution of two or more species overlaps, although they do not necessarily use the same habitat or occupy the same ecological niche. Duarte and González (2010) compiled and reunited the scarce and scattered literature on Neotropical deer, providing a great body of knowledge suitable for ecomorphological studies. However, most craniomandibular morphometric studies on Neotropical deer are aimed at identifying taxonomic or ontogenetic variations (Delupi and Bianchini 1995; González et al. 2002; Cassini et al. 2015; Gonzalez et al. 2018), and Merino et al. (2005) is the only published form-function study. Moreover, ecomorphological studies that have investigated the associations between feeding behavior and craniomandibular morphology include deer within a broad ungulate sample (e.g., Janis 1995; Mendoza and Palmqvist 2008; Cassini 2013; Fraser and Rybczynski 2014). With few exceptions, such

works are aimed at recovering taxon-free ecomorphological patterns from extant ungulates to predict feeding behavior in extinct ones (i.e., the application of Radinsky's 1987 form-function correlation paradigm). In these studies, some authors found that the mandible better reflects diet than does the cranium (see Vizcaíno et al. 2016). However, these structures (or morphological units) are linked not only by their anatomical interactions, but also by developmental and functional demands (Cuvier's correlation of parts principle; Vizcaíno and Bargo 2019). This covariation of traits is known as morphological integration, and geometric morphometric methods are particularly useful for quantifying the strength of association between morphological traits, as well as with ecological ones (Klingenberg 2009; Olsen 2017).

Neotropical deer constitute an ideal group for testing hypotheses assessing craniomandibular integration and feeding behavior. They have a recent evolutionary history and had achieved their greatest diversity by the late Pleistocene (Lujanian South American Land Mammal Age), after which all genera with large antlers (e.g., *Antifer*, *Morenelaphus*), except *Blastocerus*, became extinct and the brocket ecomorphotype became dominant (Cassini et al. 2016). If feeding behavior is a primary driver of craniomandibular shape diversification in Neotropical deer, then diet should explain most of the covariation in cranial and mandibular shape.

Materials and Methods

Specimens

We studied a sample of 194 crania and mandibles of both sexes of adult specimens representing 11 of the 17 Neotropical cervid species (Table 1). Sample size reflects specimen availability and completeness. *Mazama chunyi*, *M. bricenii*, *M. pandora*, *M. temama*, and *M. rufina* are lacking. Their biology and ecology are poorly documented (Merino and Rossi 2010), precluding ecomorphological analyses. Even so, the morphological and ecological diversity among Odocoileini is well represented. In addition, three Nearctic deer, *Alces americanus* (one female), *Odocoileus virginianus* (one female and five males), and *Rangifer tarandus* (three unsexed adults) were included in order to conduct the phylogenetic signal analyses. Materials are housed in the mammalogy collections of the following institutions: American Museum of Natural History (AMNH, New York, USA); Administración de Parques Nacionales de la Delegación Regional Patagonia (APN-DRP, Bariloche, Argentina); Museo Regional de la Reserva de Vida Silvestre "Campos Tuyú" (CDT, Buenos Aires, Argentina); Colección Félix de Azara, "Fundación Félix de Azara" (CFA, Buenos Aires, Argentina); Colección Mamíferos Lillo, "Instituto Miguel Lillo" (CML, Tucumán, Argentina); Museo Argentino de

Table 1 Neotropical deer sexed sample and diet composition for each species

Species	<i>n</i> (F/M)	body mass (kg) F/M	Diet	Fruit	Bryophyte and Pteridophyte	Gymnosperm	Dicot	Monocot
<i>Blastoceros dichotomus</i> (marsh deer)	13 / 9	100/130	M	0	0.031	0	0.423	0.546
<i>Hippocamelus antisensis</i> (taruca)	1 / 1	55/60	B	0	0.058	0.031	0.723	0.188
<i>Hippocamelus bisulcus</i> (huemul)	2 / 7	69.3/75.2	B	0.004	0.005	0.002	0.937	0.052
<i>Mazama americana</i> (red brocket)	10 / 15	30	F	0.658	0	0	0.198	0.143
<i>Mazama bororo</i> (small red brocket)	2 / 0	25	B	0.489	0	0	0.511	0
<i>Mazama gouazoubira</i> (brown brocket)	13 / 20	16.4	B	0.106	0.025	0.0001	0.834	0.036
<i>Mazama nana</i> (dwarf red brocket)	1 / 6	10	B	0.010	0	0	0.990	0
<i>Mazama nemorivaga</i> (Amazonian gray brocket)	11 / 8	14	F	0.696	0	0	0.193	0.111
<i>Ozotoceros bezoarticus</i> (pampas deer)	43 / 24	35/40	M	0.001	0	0	0.434	0.565
<i>Pudu mephistophiles</i> (northern pudu)	2 / 1	5.8	B	0.250	0	0	0.75	0
<i>Pudu puda</i> (southern pudu)	3 / 2	9.54	B	0.041	0	0.02	0.911	0.028

Notes: *N* number of specimens belonging to females (F) and males (M). Body mass (kg) following Cassini et al. (2012: appendix 2), Mattioli (2011), and Duarte and Gonzalez (2010); when sexual dimorphism exists both values are expressed with F (female) and M (male). Diet categories follow Mendoza and Palmqvist (2008): browser (B), frugivore (F), and mixed feeder (M). Dietary composition expressed as proportion of each food item was obtained following Olsen (2017) (see Materials and Methods section and Online Resource 3)

Ciencias Naturales “Bernardino Rivadavia” (MACN, Buenos Aires, Argentina); Museo de La Plata (MLP, La Plata, Argentina); Museo Provincial de Ciencias Naturales “Florentino Ameghino” (MFA-ZV, Santa Fe, Argentina); Museo de Zoología de la Universidad de São Paulo (MUZSP, São Paulo, Brazil); Núcleo de Pesquisa e Conservação de Cervídeos (NUPECCE, Jaboticabal, Brazil); and Yale Peabody Museum (YPM, New Haven, USA).

Landmark Data

The 3D landmark coordinates were acquired by GHC with a Microscribe G2L digitizer (Immersion Corporation, San José, CA, USA). The landmarks are listed in Online Resources 1–2, and shown in Fig. 1. They comprise type I (anatomic), II (mathematic), and III (semilandmarks). Both sides and the midline of the cranium were included. Semilandmarks were placed over the horny pad scar (L9–10) and anterior margin (L15–16) of the premaxilla; on the ventral (L25–27) and dorsal (L38–41) margin of the zygomatic arch; and on the dorsal (L31–32) and ventral (L35–36) margin of the orbital rim (Fig. 1a; Online Resource 1).

In the mandible 33 landmarks were digitized. Semilandmarks were placed along the dorsal aspect of the diastema (L7–8); anterior (L12–15) and posterior (L17–18) margin of the coronoid; posterior margin of the mandibular angle (masseteric scar L24–25); and the ventral margin of the alveolar region (L27–31; Fig. 1b and Online Resource 2). During digitization sessions additional semilandmarks were taken to characterize the curves, and they were reduced in number and equispaced using “resample” software of

NYCEP (Reddy et al. 2007). On the first day of digitization sessions on each collection, one specimen of each sex was digitized five times in order to assess measurement error.

Dietary Information

Information on the feeding ecology of Neotropical deer species was obtained from the published literature and theses available online, including 16 quantitative studies based on microhistological fecal and gut analyses, six quantitative studies based on direct observations, and six qualitative descriptions (Online Resource 3). Following Olsen (2017), we transformed diet composition for each deer species as relative percentages, so that frequencies would sum to 1. In order to make the categories comparable across studies, we aggregated the botanical classes into five categories: fruits (including fungi when present), bryophytes and pteridophytes, gymnosperms, dicotyledons (dicots), and monocotyledons (monocots). For each deer species, we averaged the proportions within each diet category across different habitats or seasonal values in all studies (Table 1). The use of proportions violates assumption in linear models (Warton and Hui 2011). For this reason, these five continuous dietary characters were logit-transformed prior to the analysis using the function “logit” from the R package car 2.1–6 (Fox and Weisberg 2011) with an adjustment factor of 0.1 to avoid values of zero or one. This protocol allows inclusion of dietary information, even when it is scarce and no consistent experiments were developed for all species (Olsen 2017).

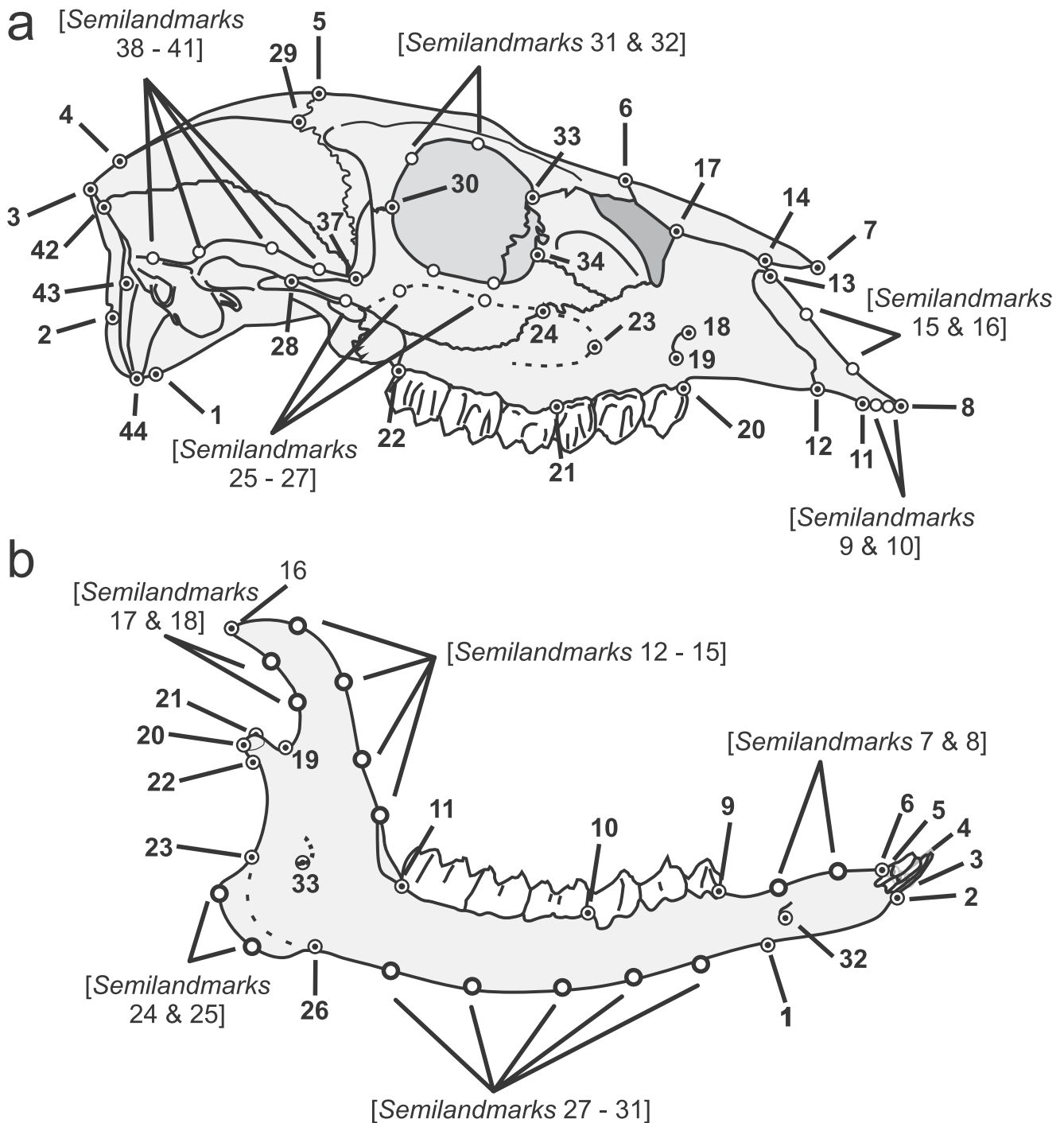


Fig. 1 Landmarks used in this study. **a** cranium and **b** mandible of *Mazama gouazoubira* (brown brocket deer) showing the landmarks on the right side and midline. Definitions listed in Online Resources 1 and 2

Geometric Morphometrics

Spatial variation that does not correspond to shape in the landmark configurations was removed using Generalized Procrustes Analysis applying rotation, translation, reflection, and scaling transformations (Rohlf 1990). Centroid size was used as a proxy for size (Dryden and Mardia 1998). To assess

the influence of phylogeny on both craniomandibular shape and size on the one hand and on continuous dietary characters on the other hand, two evolutionary scenarios were considered (Online Resource 4). The first scenario was obtained from the 10KTrees website version 1 (Arnold et al. 2010). The northern pudu (*Pudu mephistophiles*) was added as a sister group of Rangiferini + Odocoileini based on the phylogeny of

Heckeberg et al. (2016). The second scenario was the Cetartiodactyla tree by Zurano et al. (2019), pruned to consider only the species present in this study. In this scenario, the northern pudu is the sister group of Blastocercina sensu Heckeberg et al. (2016). The branch weighted squared-change parsimony method was used to reconstruct the ancestral stages of internal nodes (Maddison 1991), and the phylogenetic signal was tested by a permutation test (with squared-change parsimony) with 10,000 rounds of permutation test. Independent contrasts of shape and size were stored for subsequent analyses.

The Partial Least Squares analysis (PLS) was used to find correlated pairs of linear combinations between two block sets that maximize covariation between them (Klingenberg 2013). The PLS produces vectors of shape variation and individual scores that account for major covariation between the two blocks, and provides an estimate of covariation (R^2) based on Pearson's correlation coefficient. Significance of each PLS axis was calculated by 10,000 rounds of permutation test.

Evolutionary craniomandibular integration (i.e., cranium Block-1 and mandible Block-2) was studied using PLS on both the superimposed coordinates and the independent contrasts (Klingenberg and Marugán-Lobón 2013). The extent and significance of the association between each significant PLS and log-transformed centroid size was assessed via a permutation test with 10,000 rounds.

Following Merino et al. (2005), two ecomorphological patterns of covariation were evaluated in: (1) Neotropical deer as a whole and (2) small and large Neotropical deer. A cut-off point between 30 and 35 kg was applied for distinguishing the small species without sexual size dimorphism from large species with reported size dimorphism. The correlation between cranial shape and diet, and between mandibular shape and diet, were assessed via two-block PLS. Cranial or mandibular shape (i.e., landmark configurations) and continuous diet characters (i.e., the logit-transformed diet proportions matrix) were defined as Block-1 and Block-2, respectively.

All morphometric analyses produce vectors in shape space (Drake and Klingenberg 2008). Angular comparisons of vector directions were performed to evaluate the similarity in shape changes between them. The angles between these vectors were compared under the null hypothesis of orthogonality. When these angles are close to zero the shape change vectors are similar and consequently explain a similar shape change (Klingenberg and Marugán-Lobón 2013).

All morphometric analyses were performed in MorphoJ 1.07a software (Klingenberg 2011). The visualization and graphics were made using the *Morpho* 2.6 R-package (Schlager 2017; R Core Team 2018), which allows visualizing shape changes using color patterns.

Data Availability

All data generated during our analyses in the current study are available from the corresponding author on reasonable request.

Results

Evolutionary Integration

The analyses showed no significant phylogenetic signal in cranial and mandibular shape (Procrustes coordinates) or size (i.e., log-transformed centroid size). The exception was the cranial shape evaluated on the phylogenetic hypothesis of Zurano et al. (2019) (Table 2). Similar results were found for continuous dietary characters for both phylogenetic hypotheses (Table 2).

The PLS analysis on the Capreolinae species (PLSca) showed that the first two pairs of PLS explain about 91% of covariation (Table 3). The shape change vectors associated with the first pair were very similar to those of analysis on the independent contrasts obtained on the Zurano et al. (2019) phylogeny (PLSicz; Online Resources 5, 6). The angular comparison showed an angle between vectors of 12.139° for cranium (Block-1) and 13.831° for mandible (Block-2), both p -values <0.00001 . In addition, scores of the first pair of axes (PLSca1) of the two blocks correlated significantly and positively with cranium and mandible log-transformed centroid size ($R^2 = 0.75$ and $R^2 = 0.56$ respectively for Block-1 and Block-2, both p value <0.0001 ; see Table 3).

The PLSca1 vectors were visualized as surface plus thin plate spline (TPS) gridline deformations (Fig. 2). The shape changes associated with Block-1 ranged from a short but broad cranium (negative values) to a long and slender cranium (positive values, Fig. 2a). Consequently, small forms were characterized by the muzzle tip placed above the occlusal plane, short but high rostrum, broad palate, similar premolar and molar row lengths, anteriorly displaced large orbits, a laterally expanded zygomatic arch delimiting a large temporal fossa, and a posteriorly displaced occiput and foramen magnum (negative end, Fig. 2a). By contrast, large forms were characterized by the muzzle tip placed below the occlusal plane, long and low rostrum, narrow palate, premolar row shorter than molar row, posteriorly displaced small orbits, medially compressed zygomatic arch delimiting a small temporal fossa, and an anteriorly displaced occiput and foramen magnum (positive end, Fig. 2a). These shape changes correlated to a range of shapes in Block-2 from a mandible with an acute angle between the alveolar region and the ascending ramus on the negative end to an obtuse angle on the positive end. In correspondence with cranial shape changes, small forms were characterized by a mandible with robust symphysis with

Table 2 Phylogenetical signal tests for shape, size, and ecological data sets

	Cranial shape	Cranial log(CS)	Mandible shape	Mandible log(CS)	Fruit	Bryo-Pterid	Gymno	Dicot	Monocot
Scenario 1									
Tree length	0.0563	1.133	0.0272	1.389	7.573	0.167	0.0531	11.285	4.852
<i>p</i> value	0.2308	0.4436	0.6206	0.4370	0.1844	0.6265	0.3548	0.9678	0.2281
Scenario 2									
Tree length	0.0512	1.0011	0.0229	1.231	9.227	0.158	0.0567	10.0871	5.7919
<i>p</i> value	0.0262*	0.1355	0.0506	0.1279	0.2722	0.3508	0.4273	0.7152	0.3924

Notes: Scenario 1: 10ktree consensus; scenario 2: Zurano et al. (2019); log(CS) – log-transformed centroid size; Bryo-Pterid - bryophytes and pteridophytes; Gymno – gymnosperms; diet continuous character test performed on logit transformed values; tree length based on weighted squared-change parsimony; *p* values after 10,000 rounds of permutation; value marked by asterisk (*) significant at 0.05 level

incisor alveoli placed above the occlusal plane, short diastema, curved and high alveolar region, more developed coronoid process, posteriorly directed masseteric fossa, and comparatively lower position of the condyle (Fig. 2b). Conversely, large forms were characterized by a mandible with gracile symphysis with incisor alveoli placed below the occlusal plane, long diastema, straight and low alveolar region, less developed coronoid process, anteriorly directed masseteric fossa and comparatively higher position of the condyle (Fig. 2b; Online Resource 5).

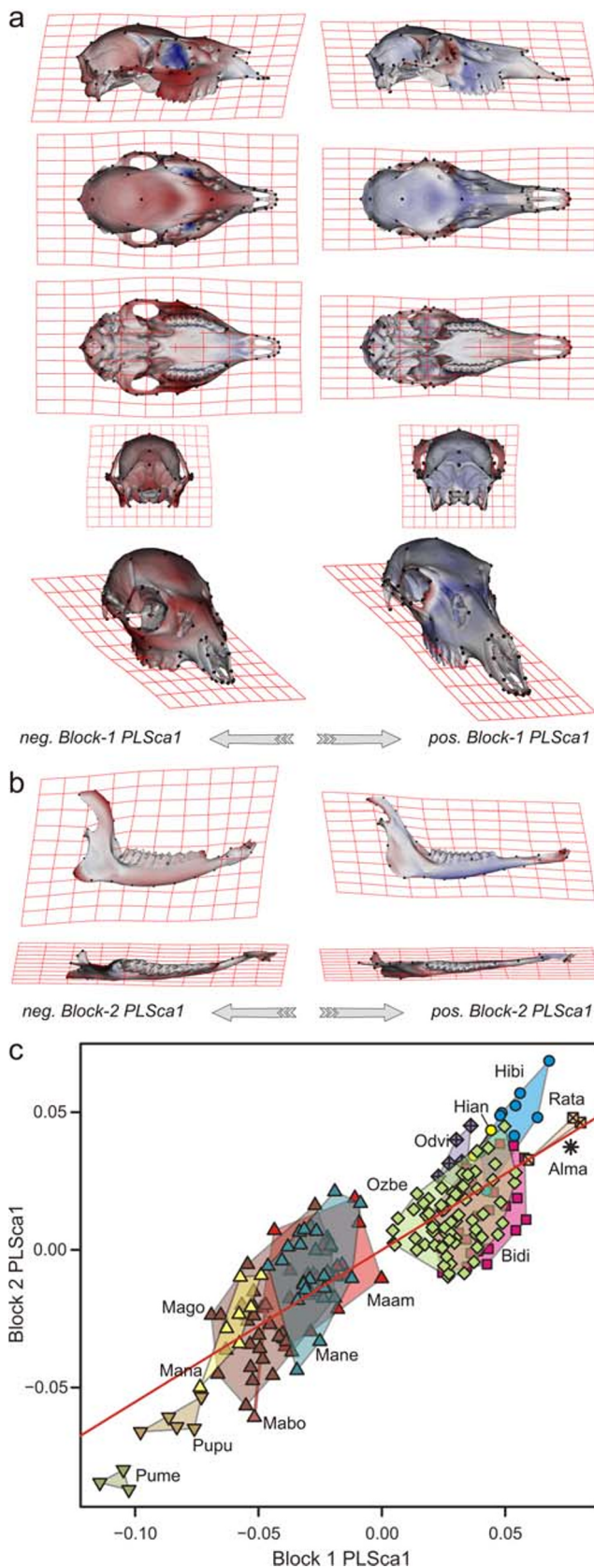
The PLSca1 scores showed a high correlation between blocks ($r = 0.85$, $p < 0.00001$ after 10,000 rounds of permutation tests). The pudus and brockets (i.e., small deer) are in the

double negative quadrant, showing a right point cloud with a common pattern of covariation mainly associated with a brachycephalic cranium with robust mandible (Fig. 2c). Conversely, the large deer including the Neotropical pampas deer, marsh deer, and huemuls, and the Nearctic caribou, white-tailed deer, and moose clustered in a small region on the double positive quadrant, slightly displaced to positive values of Block-1 showing a pattern of covariation mainly associated with a dolicocephalic cranium with gracile mandibles (Fig. 2c). The dimensions displayed a clear distinction between the small and large species, suggesting a slightly different pattern of covariation between these two groups regardless of sex or their phylogenetic relationships.

Table 3 Partial Least Squares analysis for each data set

Data set	Pair of axes	Singular value	S.v. <i>p</i> value	% Total covar.	Correlation	Corr. <i>p</i> value
Capreolinae	PLSca1	0.001009	<0.0001	90.610	0.85502	<0.0001
Cr and Md	PLSca2	0.00022315	<0.0001	4.432	0.72998	<0.0001
independent	PLSicz1	0.0003408	0.0005	82.111	0.92062	0.0002
contrast Cr and Md	PLSicz2	0.0001411	0.0023	14.067	0.90137	0.0021
Neotropical deer	PLScd1	0.04409008	<0.0001	93.993	0.84457	<0.0001
Cr shape and diet	PLScd2	0.01110595	<0.0001	5.964	0.65176	<0.0001
Neotropical deer	PLSmd1	0.01934187	<0.0001	76.520	0.63990	<0.0001
Md shape and diet	PLSmd2	0.01068946	<0.0001	23.372	0.57772	<0.0001
Small deer	PLScd1	0.03067931	<0.0001	99.763	0.71940	<0.0001
Cr and diet	PLSmd1	0.02731151	<0.0001	99.695	0.63227	<0.0001
Small deer	PLSmd1	0.02731151	<0.0001	99.695	0.63227	<0.0001
Md and diet	PLSmd1	0.02731151	<0.0001	99.695	0.63227	<0.0001
Large deer	PLSlcd1	0.01363645	<0.0001	98.224	0.84822	<0.0001
Cr and diet	PLSlcd1	0.01363645	<0.0001	98.224	0.84822	<0.0001
Large deer	PLSlmd1	0.01220972	<0.0001	98.957	0.73461	<0.0001
Md and diet	PLSlmd1	0.01220972	<0.0001	98.957	0.73461	<0.0001

Notes: PLS: Partial Least Squares; S.v. *p* value: permutation test on Singular values; % Total covar.: Total covariance percent; Correlation: Pearson correlation coefficients between PLS scores of Block-1 and Block-2; Corr. *p* value: permutation test on correlation values from the PLS scores; Cr: cranium; Md: mandible; PLS subindices: (ca) the whole Capreolinae sample, (icz) independent contrast from Zurano et al. (2009) phylogeny, (cd) cranial shape and diet, (md) mandibular shape and diet, (scd) cranial shape and diet in small Neotropical deer, (smd), mandibular shape and diet in small Neotropical deer, (lcd) cranial shape and diet in large Neotropical deer and (lmd) mandibular shape and diet in large Neotropical deer



◀ **Fig. 2** PLSca of Capreolinae specimens. **a** thin plate spline gridlines and meshes of cranium shape (Block-1) of negative and positive most first pair of PLS; **b** thin plate spline gridlines and meshes of mandibular shape (Block-2) of negative and positive most first pair of PLS; **c** taxa distribution on the morphospace depicted by the two first PLS dimensions. Reference: *Alces americanus* (asterisk - Alma); *Blastocercus dichotomus* (squares - Bidi); *Hippocamelus* spp. (circles - Hian, *H. antisensis* and Hibi, *H. bisulcus*); *Mazama* spp. (triangles - Maam, *M. americana*; Mabo, *M. bororo*; Mago, *M. gouazoubira*; Mana, *M. nana*; Mane, *M. nemorivaga*); *Odocoileus virginianus* (crossed rhombus - Odvi); *Ozotoceros bezoarticus* (rhombus - Ozbe); *Pudu* spp. (inverted triangles - Pume, *P. mephistophiles*; Pupu, *P. puda*); and *Rangifer tarandus* (crossed squares - Rata)

Ecomorphology of Neotropical Deer

The PLS analysis on both cranium and mandible of Neotropical deer showed a significant relationship between shape and diet. The PLS analysis on the cranial and mandibular shape indicated that the first pair of PLS explains about 94% and 76% of covariation, respectively (PLScd1 and PLSmd1, Table 3). In both analyses the shape change vectors associated with the first block (i.e., cranium and mandible; Online Resource 7) were similar to the respective Block-1 and Block-2 of the Capreolinae PLSca1 (angle between vectors: 17.22° for cranium and 19.591° for mandible; both $p < 0.00001$). The Block-2 PLS coefficients of the five diet categories for each analysis were quite similar. In both, the monocot items showed similar high negative values (ca. -0.77) and the fruit items very similar high positive value (ca. 0.59 for cranium and ca. 0.57 for mandible). While the PLScd1 scores showed a very high and significant correlation between Block-1 and Block-2 ($r = 0.845$, $p < 0.00001$; Table 3), the scores of first pair of PLS for mandible and diet (PLSmd1) showed lower but significant correlation ($r = 0.6399$; $p < 0.00001$; Table 3). The morphospace of both analyses are strongly similar and lack any sexually dimorphic pattern (Online Resource 7). Among the large Neotropical deer, the mixed feeders *Ozotoceros bezoarticus* and *Blastocercus dichotomus* fall into the double negative quadrant, and the browser *Hippocamelus* spp. on negative values of Block-1 and near the zero and positive values of Block-2 scores (Online Resource 7). The small deer, the browser *Pudu* spp. and *Mazama* spp., including browsers and frugivores, are in the double positive quadrant.

Ecomorphological Integration in Small Deer

The PLS analysis on both the cranium and mandible of small deer showed a significant relationship between shape and diet. Both PLS analyses showed that the first pair of PLS explains about 100% of covariation (PLSscd1 and PLSsmd1, respectively; Table 3). The shape changes associated with the PLSscd1 vector of Block-1 (Fig. 3a) ranged from a short

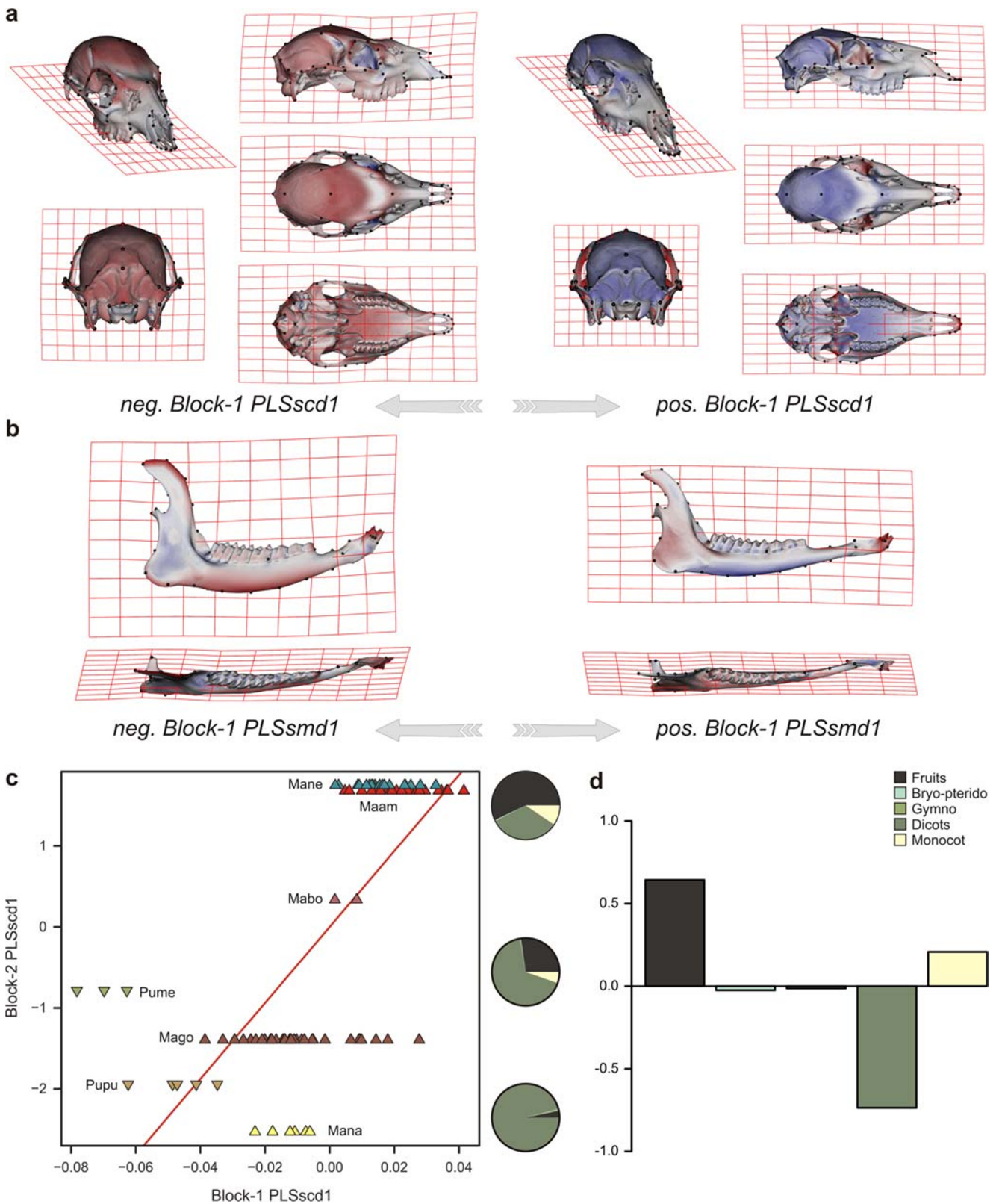


Fig. 3 PLS of cranial and mandibular shape (Block-1) vs logit continuous dietary characters (Block-2) in small deer specimens. **a** thin plate spline gridlines and meshes of cranium shape (Block-1) of negative and positive most first pair of PLSScd; **b** thin plate spline gridlines and meshes of mandibular shape (Block-1) of negative and positive most first pair of

PLSsmd; **c** taxa distribution on the morphospace depicted by the two first PLS dimensions of cranium analysis (PLSscd), with pie charts depicting dietary composition near extreme and midpoint y-axis values; and **d** pairwise correlation coefficients between diet PLS axis and each dietary category (logit-transformed) for PLSscd. References as in Fig. 2

and high cranium with the muzzle tip above the occlusal plane, orbits placed above the masseter's origin, laterally expanded and dorsally curved zygomatic arch, wide cranial vault, and posteriorly directed occiput and foramen magnum (on the negative end) to a short but low cranium with the muzzle tip below the occlusal plane, orbits placed towards the third molar, medially compressed and straight zygomatic arch, narrow cranial vault, and anteriorly directed occiput and foramen magnum (on the positive end).

Shape changes associated with the PLSsmd1 vector of Block-1 (Fig. 3b) ranged from a mandible with a curved diastema and high alveolar region, ventrally placed distal margin of angular process, and high and anteriorly directed coronoid process (on the negative end) to a mandible with a straight diastema, low alveolar region, dorsally placed angular process, and low and posteriorly directed coronoid process (on the positive end).

The Block-2 PLS coefficients of the five diet categories for each analysis were very similar. In both cranial and mandibular PLS the dicot items showed similar high negative values (ca. -0.73) and the fruit items high positive values (ca. 0.64). While the PLSscd1 scores showed a high and significant correlation between Block-1 and Block-2 ($r = 0.719$, $p < 0.00001$; Table 3), the PLSsmd1 scores showed lower but significant correlation ($r = 0.632$; $p < 0.00001$; Table 3). In both analyses the morphospaces looked quite similar but in mandible Block-1 PLS axis showed greater dispersion. There was no sexual dimorphism pattern in the morphospace depicted by the first PLSscd and PLSsmd dimensions. The browser pudus and brockets *Mazama gouazoubira* and *M. nana* are in the double negative quadrant, and the frugivorous brockets *M. nemorivaga* and *M. americana* in the double positive quadrant (see Fig. 3c and d for PLSscd).

Ecomorphological Integration in Large Deer

The PLS analysis of both the cranium and mandible of large deer showed a significant relationship between shape and diet. Both PLS analyses showed that the first pair of PLS explains about 98% covariation (PLSlcd1 and PLSlmd1, respectively, Table 3). The PLSlcd1 vector of Block-1 shape changes (Fig. 4a) ranged from a cranium with a flexion between the rostrum and the orbital region plus cranial vault, muzzle tip above the occlusal plane, ventral and anteriorly placed large orbits and infraorbital foramen, robust zygomatic arch, and posteriorly directed occiput and foramen magnum (on the negative end) to a cranium with flexion between the orbitofacial region and the cranial base and vault, muzzle tip above the occlusal plane, dorsal and posteriorly placed orbits and infraorbital foramen, gracile zygomatic arch, and anteriorly oriented occiput and foramen magnum (on the positive end).

The shape changes associated with PLSlmd1 vector of Block-1 (Fig. 4b) ranged from a mandible with a curved and high alveolar region (particularly along the molar region), more developed angular process, and anteriorly directed coronoid process on the negative end to a mandible with a straight diastema and alveolar region, less developed angular process, and posteriorly directed coronoid process (on the positive end).

The Block-2 PLS coefficients of the five diet categories for each analysis showed very similar values. In both the cranial and mandibular PLS the monocot items showed similar high negative values (ca. -0.72) and the dicot items very high positive values (ca. 0.69). While the PLSlcd1 scores show a very high and significant correlation between Block-1 and Block-2 ($r = 0.848$, $p < 0.00001$; Table 3), the PLSlmd1 scores showed lower but significant correlation ($r = 0.734$; $p < 0.00001$; Table 3). In both analyses, the morphospace depicted by first dimensions of these PLS looked quite similar and clustered the mixed feeders *Ozotoceros bezoarticus* and *Blastocerus dichotomus* towards the negative quadrant, while the browsers *Hippocamelus* spp. clustered towards positive scores (see Fig. 4c and d for PLSlcd). No sexual dimorphic pattern was detected.

Discussion

Our study suggests that feeding ecology in Neotropical deer has strongly influenced craniomandibular shape and size diversification. There is a remarkable convergence between the brockets in their feeding behavior (e.g., high proportion of fruit in their diet) and morphology (brachycephalic cranium with robust mandible). Conversely, marsh and pampas deer share craniomandibular traits (e.g., large attachment areas for masseter plus pterygoid muscles) related to monocotyledon consumption. It is noteworthy how close the morphology reflects the actual diet instead of the phylogeny, suggesting a high correspondence between fundamental and realized niche (see Vizcaíno et al. 2016 and references there in). In addition, as noted in Merino et al. (2005), sex differences were not apparent in any of the analyses performed. Phylogenetic signal was not significant in almost all the morphogeometric data and continuous diet characters. Similar results were obtained using the independent contrast, suggesting a lack of phylogenetic constraints, conversely to what was proposed for shape data of other ungulates and mammalian groups (e.g., Cardini and Elton 2008; Barčiová 2009; Cassini 2013).

Evolutionary Integration

Size emerges as one important factor modeling slightly different patterns of covariation in small and large Neotropical deer. Results were similar between the PLS analysis of the entire

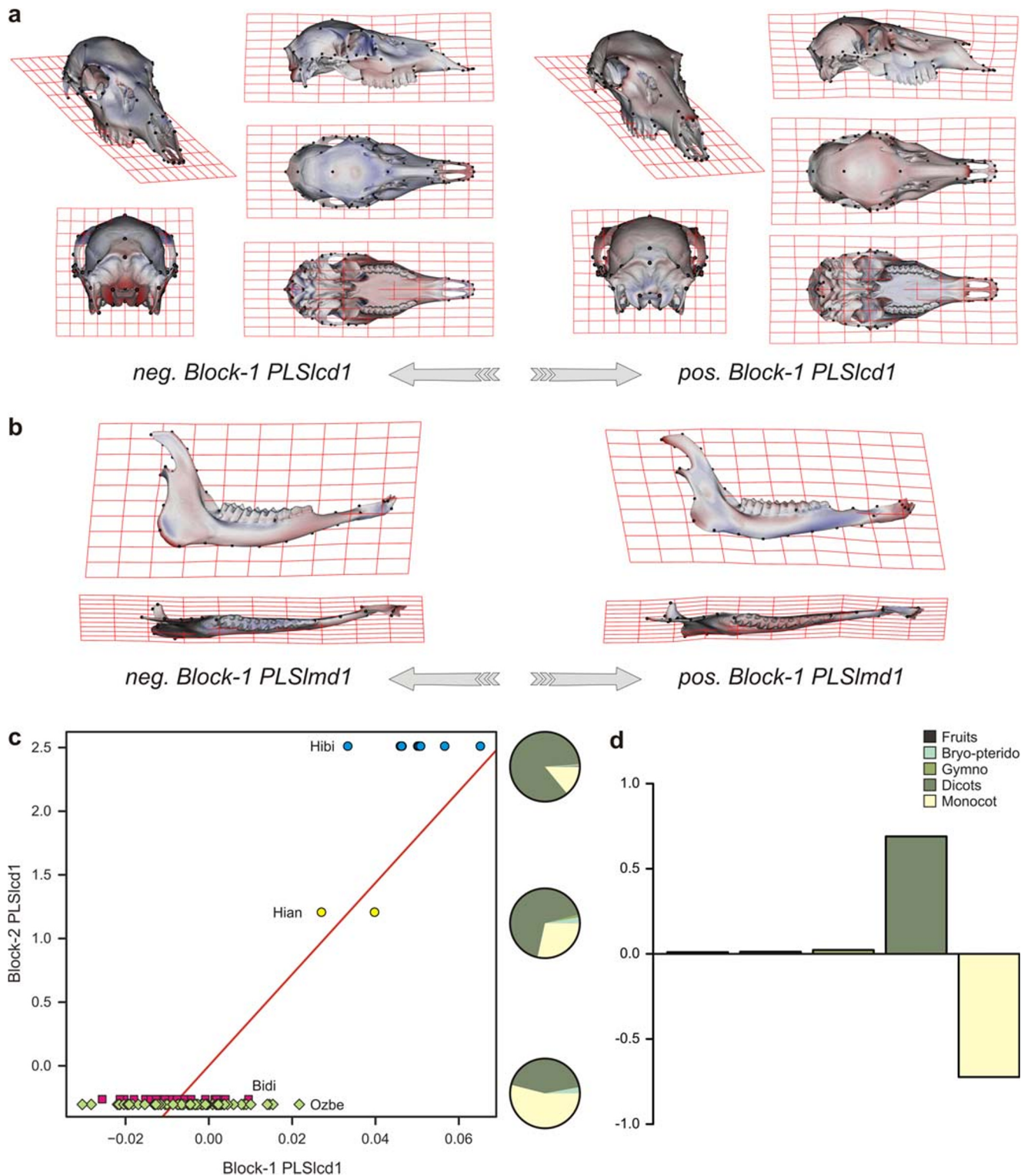


Fig. 4 PLS of cranial and mandibular shape (Block-1) vs. logit continuous dietary characters (Block-2) in large deer specimens. **a** thin plate spline gridlines and meshes of cranium shape (Block-1) of negative and positive most first pair of PLS1cd; **b** thin plate spline gridlines and meshes of mandibular shape (Block-1) of negative and positive most first pair of

PLS1md; **c** taxa distribution on the morphospace depicted by the two first PLS dimensions of cranium analysis (PLS1cd), with pie charts depicting dietary composition near extreme and midpoint y-axis values; and **d** pairwise correlation coefficients between diet PLS axis and each dietary category (logit-transformed) for PLS1cd. References as in Fig. 2

Capreolinae sample and independent contrast of both phylogenetic hypotheses (i.e., PLSca and PLSic; Online Resource

6). In the morphospace depicted by the first dimensions of these PLS (Fig. 2), it clearly emerges that the morphological

covariation pattern shared by Capreolinae ranges from a brachycephalic cranium with robust mandible to a dolicocephalic cranium with a gracile mandible (Fig. 2a-b; Online Resource 5). The log-transformed centroid size explains 75% and 56% of cranial and mandibular variation, respectively (see Results), suggesting that craniomandibular integration could be explained by allometric scaling (note that our sample includes the pudu and moose, the smallest and largest extant cervids). In accordance with Cassini (2013), many ungulate lineages shared common allometric shape changes in both cranium (e.g., small forms were characterized by a narrow muzzle, short rostrum and large temporal fossa versus a wide muzzle, long rostrum and small temporal fossa, i.e., brachycephalic vs. dolicocephalic) and mandible (small forms are characterized by an acute angle between the alveolar region and the ascending ramus, whereas larger forms are characterized by an obtuse angle, i.e., robust vs. gracile). A similar allometric pattern was reported as appearing convergently in many other mammal groups (e.g. antelopes, bats, mongooses, and squirrels, see Cardini and Polly 2013). In addition, Janis and Theodor (2014) indicated that within Ruminantia there are many highly homoplastic morphological features related to functional similarities but not to phylogeny, and Neotropical deer are not an exception. Recent molecular phylogenetic hypotheses (Heckeberg et al. 2016; Zurano et al. 2019) confirmed the evolutionary scenario of Duarte et al. (2008), in which brachycephalic morphology (e.g., brockets) evolved at least twice. Therefore, allometry would be an influential factor shaping the evolutionary craniomandibular integration in deer.

Ecomorphology of Neotropical Deer

In addition to the craniomandibular covariation pattern explained by allometric scaling, the Neotropical deer species analyzed here show shape changes that were found to be related to diet composition. Surprisingly, as is shown by angular comparison, the shape changes were similar to the evolutionary integration analyses (compare Fig. 2 with online Resources 6 and 7 shape changes). The covariation between shape variation and diet was higher for the cranium (94%) than for the mandible (76%; Table 3; Online Resource 7). This contradicts the accepted hypothesis that the mandible better reflects masticatory function than the cranium (Janis 1995; Vizcaino et al. 2016, and references therein).

In both the cranium and mandible, axes of correlation were consistent with differences at the level of the primary plant-food preference (i.e., monocot vs. fruit). However, both shape changes are quite similar to the craniomandibular integration in the PLS of Capreolinae (angular between vectors of $\sim 17^\circ$ for cranium and 19° for mandible). Both covariation morphospaces reveal that the small and large Neotropical deer have slightly different covariation patterns (Online Resource

7). The most conspicuous features correlated with more than 50% of monocots in diet were: a long rostrum, braincase flexed on the facial axis, narrow palate, depth of the facial region below the orbit, small temporal fossa (in the cranium); and a long diastema, short premolar row, deep masseteric fossa and high articular process with a short and posteriorly oriented coronoid process (in the mandible). As also noted by Greaves (2012), this morphology emphasizes the anteroposterior resultant force of jaw musculature, rendering it more horizontal (because the masseter and pterygoid are large; Radinsky 1985), with a shorter component of temporal muscle in the stroke phase in comparison with pterygoid-masseteric component. In agreement with Merino et al. (2005), these traits are shared mainly by pampas deer and marsh deer, which are also very selective on the plant parts they consume (see Duarte and González 2010). According to Janis (2007), cervids never became specialized grazers (i.e., >90% of monocot) or developed highly hypsodont teeth as bovids. However, the above mentioned features were demonstrated to be related to grass consumption in grazing and mixed feeding African bovids (Spencer 1995; Janis 2000; Clauss et al. 2008). Thus, this pattern suggests that grass consumption is correlated with distinctive skull features, even if grass is not the dominant item in the diet.

Traits condensed in the opposite extreme of the morphospace, i.e., short and high rostrum, anteriorly directed orbits, wide zygomatic arch, and mandible with short diastema and right angle between the alveolar region and the angular process, among others, are shared by the red-brocket and the Amazonian grey-brocket deer, and correlates with a high percentage of fruit in the diet (i.e., >60%; See Online Resource 7). While most ungulates have an anteriorly-directed jaw musculature resultant (Greaves 1991), these traits seems to favor a more posteriorly directed vector, rendering it more vertical, because of the great development of the temporal fossa and muscle (Greaves 2012). This arrangement brings the third molar closer to the craniomandibular joint and emphasizes the component of the temporal muscle during the stroke phase (Greaves 2012). In addition, a lower condyle leads to reduced muscle stretch, which can enable a wider gape (Herring and Herring 1974). This scheme seems be coherent with a high percentage (both regular and seasonal) of fruit in the diet (Table 1).

Ecomorphological Integration in Small Deer

Size emerges as one important factor that modeled patterns of covariation within small deer. The correlation of shape variation and diet was extremely high in both the cranium and mandible (ca. 100%, respectively; Fig. 3; Table 3). The small deer follow the general allometric pattern described above for the entire Capreolinae sample but within a general brachycephalic-robust mandible morphotype (compare Figs. 2 and 3 shape

changes). Surprisingly, within the small deer the shape change gradient was inverted, as the *Pudu* spp. consume more dicots (browser) than *Mazama nemorivaga* and *M. americana*, which consume more fruits. The covariation morphospaces reveal inconsistencies in shape and diet correlation that might be explained by the scarcity and low-grade information on diet. For example, *Mazama nana* is similar to *M. bororo* in size, habitat use, and Block-1 (shape) scores, and it would thus be expected to have similar fruit content (45%, Table 3), rather than the higher percentage of dicots noted here. Some authors consider that further studies are required to provide a better understanding of the ecology of these species (see Duarte and González 2010). Indeed, Radinsky claimed on the needs of including direct field or lab observations of behavior or responses to environmental factors in adaptation research programs (see Vizcaíno and Bargo 2019).

Ecomorphological Integration in Large Deer

The observed correlation between cranial and mandibular shape and diet within the large deer appears to be explained not by allometric scaling, but rather by the monocot-dicot gradient. The correlation of shape variation and diet was slightly higher in the mandible than cranium (ca. 100% and 98%, respectively; Fig. 4; Table 3). In both, axes of correlations are consistent with differences at the level of the primary plant-food preference (i.e., dicots), as in the entire Capreolinae sample. There seems to be a gradient in diet composition from *Hippocamelus bisulcus*, feeding primarily on dicots (>90%), to the mixed feeders *Ozotoceros* and *Blastoceros*, consuming lower proportions of dicots (ca. 40%; Table 3). Monocot consumption greater than 50% is associated with flexion between the rostrum and orbital region, a posteriorly oriented occiput, and a robust zygomatic arch 4a in the cranium, and a high curved alveolar region, expanded angular process, and masseteric fossa providing more attached surface area for masseter and pterygoid muscles in the mandible. Conversely, a high dietary consumption of dicots is associated with flexion between the orbit and basicranium, an anteriorly oriented occiput and gracile zygoma (Fig. 4b), and a slender mandible with a straight diastema, an alveolar region forming an obtuse angle with the ascending ramus, and a small masseteric fossa. This gradient of shape variation associated with monocot to dicot dominated diets (Fig. 4c-d) is consistent with the convergent functional complex related to habitat/diet and tooth dimensions described by Cassini (2013) and Fraser and Theodor (2011) for extant and extinct ungulates.

Conclusions

The covariation between craniomandibular features and feeding behavior, investigated with continuous dietary

characters and modern geometric morphometry techniques, reveals morphological convergences within small and large Neotropical deer that are explained by a complex interplay of allometric trends and biomechanically significant features. Notable is the high correspondence between morphology and feeding behavior in Neotropical cervids, which emerges apparently from the novel approach of considering diet as a continuous character rather than as discrete categories. The association of craniomandibular traits with diets high in monocot, fruit, or dicot plant material underscores the importance of relative toughness of food items as an ecological factor shaping skull variation. Radinsky (1987) highlighted remarkable convergences between distant lineages of herbivorous mammals; here we postulate some between Neotropical cervids with African bovids. Although cervids never reached the same degree of dietary specialization as bovids, growing evidence from several research fields will contribute to understanding the adaptive role of craniomandibular shape in the recent evolutionary history of deer in the Neotropics.

Acknowledgments We thank N. Simmons (AMNH), H. Pastore and E. Ramilo (APN-DRP), M. Beade (CDT), S. Bogan (CFA), R. Barquez (CML), Pablo Teta (MACN), D. Verzi and I. Olivares (MLP), A. Pautaso (MFA), M. De Vivo (MUZSP), J.M. Barbanti Duarte (NUPECCE), and K. Zyskowski (YPM) for access to mammalogy collections; the organizers of the XXXI Jornadas Argentinas de Mastozoología, La Rioja, Argentina, A. Chemisquy and F. Prevosti for allowing us organizing the symposium: “El paradigma de correlación forma-función en mastozoología: un tributo a Leonard Radinsky (1937–1985)”; S. Vizcaíno and R. Fariña for having introduced us to Radinsky’s delightful text as students; S. Bargo, N. Milne, N. Muñoz, and M. Merino for fruitful discussions on form-function, geometric morphometrics, and deer that inspired this manuscript; G. De Iuliis and the reviewers whose comments greatly enhanced this manuscript. This is a contribution to the projects Universidad Nacional de Luján CDDCB 650/14 and 016/19; and Agencia Nacional Promoción Científica y Tecnológica PICT-2015-2389.

References

- Arnold C, Matthews LJ, Nunn CL (2010) The 10kTrees website: a new online resource for primate phylogeny. *Evol Anthropol* 19:114–118
- Barčiová L (2009) Advances in insectivore and rodent systematics due to geometric morphometrics. *Mammal Rev* 39:80–91
- Cardini A, Elton S (2008) Does the skull carry a phylogenetic signal? Evolution and modularity in the guenons. *Biol J Linn Soc* 93: 813–834
- Cardini A, Polly PD (2013) Larger mammals have longer faces because of size-related constraints on skull form. *Nat Commun* 4:2458
- Cassini GH (2013) Skull geometric morphometrics and paleoecology of Santacrucian (late early Miocene; Patagonia) native ungulates (Astrapotheria, Litopterna, and Notoungulata). *Ameghiniana* 50: 193–216
- Cassini GH, Flores DA, Vizcaíno SF (2015) Postnatal ontogenetic scaling of pampas deer (*Ozotoceros bezoarticus celer*: Cervidae) cranial morphology. *Mammalia* 79:69–79

- Cassini GH, Muñoz NA, Merino ML (2016) Evolutionary history of South American Artiodactyla. In: Agnolin FL, Lio GL, Brissón Egli F, Chimento NR, Novas FE (eds) *Historia evolutiva y paleobiogeográfica de los vertebrados de América del Sur*. Contribuciones del MACN:6, Buenos Aires, pp 673–689
- Cassini GH, Vizcaíno SF, Bargo MS (2012) Body mass estimation in early Miocene native South American ungulates: a predictive equation based on 3D landmarks. *J Zool* 287:53–64
- Clauss M, Kaiser T, Hummel J (2008) The morphophysiological adaptations of browsing and grazing mammals. In: Gordon IJ, Prins HHT (eds) *The Ecology of Browsing and Grazing*. Springer-Verlag, Berlin, pp 47–88
- Delupi LH, Bianchini JJ (1995) Análisis morfológico comparado de los caracteres craneo-faciales en el ciervo de las pampas *Odocoileus bezoarticus* y formas relacionadas. *Physis* 50:23–36
- Drake AG, Klingenberg CP (2008) The pace of morphological change: historical transformation of skull shape in St Bernard dogs. *Proc R Soc Lond B Bio* 275:71–76
- Dryden IL, Mardia KV (1998) *Statistical Shape Analysis*. John Wiley & Sons, Chichester
- Duarte JMB, González S (2010) Neotropical Cervidology. *Biology and Medicine of Latin American Deer*. FUNEP & IUCN, Jaboticabal
- Duarte JMB, González S, Maldonado JE (2008) The surprising evolutionary history of South American deer. *Mol Phylogenet Evol* 49:17–22
- Fox J, Weisberg S (2011) *An R Companion to Applied Regression*. Sage, Los Angeles
- Fraser D, Rybczynski N (2014) Complexity of ruminant masticatory evolution. *J Morphol* 275:1093–1102
- Fraser D, Theodor JM (2011) Anterior dentary shape as an indicator of diet in ruminant artiodactyls. *J Vertebr Paleontol* 31:1366–1375
- González S, Álvarez-Valín F, Maldonado JE (2002) Morphometric differentiation of endangered pampas deer (*Ozotoceros bezoarticus*), with description of new subspecies from Uruguay. *J Morphol* 84:1127–1140
- González S, Bonfim Mantelatto AM, Duarte JMB (2018) Craniometrical differentiation of gray brocket deer species from Brazil. *Rev Mus Arg Cien Nat ns* 20:179–193
- Greaves WS (1991) The orientation of the force of the jaw muscles and the length of the mandible in mammals. *Zool J Linnean Soc* 102:367–374
- Greaves WS (2012) *The Mammalian Jaw: A Mechanical Analysis*. Cambridge University Press, Cambridge
- Gutiérrez EE, Helgen KM, McDonough MM, Bauer F, Hawkins MTR, Escobedo-Morales LA, Patterson BD, Maldonado JE (2017) A gene-tree test of the traditional taxonomy of American deer: the importance of voucher specimens, geographic data, and dense sampling. *ZooKeys* 697:87–131
- Heckeberg NS, Erpenbeck D, Wörheide G, Rössner GE (2016) Systematic relationships of five newly sequenced cervid species. *PeerJ* 4:e2307
- Herring SW, Herring SE (1974) The superficial masseter and gape in mammals. *Am Nat* 108:561–576
- Janis CM (1995) Correlations between craniodental morphology and feeding behavior in ungulates: reciprocal illumination between living and fossil taxa. In: Thomason JJ (ed) *Functional Morphology in Vertebrate Paleontology*. Cambridge University Press, Cambridge, pp 76–98
- Janis CM (2000) Patterns in the evolution of herbivory in large terrestrial mammals: the Paleogene of North America. In: Sues HD, Labandiera C (eds) *Evolution of Herbivory in Terrestrial Vertebrates*. Cambridge University Press, Cambridge, pp 168–222
- Janis CM (2007) Artiodactyl paleoecology and evolutionary trends. In: Prothero DR, Foss SE (eds) *The Evolution of Artiodactyls*. John Hopkins University Press, Baltimore, pp 292–302
- Janis CM, Theodor JM (2014) Cranial and postcranial morphological data in ruminant phylogenetics. *Zitteliana* 32:15–31
- Kay RF (2019) Leonard B. Radinsky (1937–1985), radical biologist. *J Mammal Evol* <https://doi.org/10.1007/s10914-019-09479-4>
- Klingenberg CP (2009) Morphometric integration and modularity in configurations of landmarks: tools for evaluating a priori hypotheses. *Evol Dev* 11:405–421
- Klingenberg CP (2011) MorphoJ: an integrated software package for geometric morphometrics. *Mol Ecol Resour* 11:353–357
- Klingenberg CP (2013) Cranial integration and modularity: insights into evolution and development from morphometric data. *Hystrix* 24:43–58
- Klingenberg CP, Marugán-Lobón J (2013) Evolutionary covariation in geometric morphometric data: analyzing integration, modularity, and allometry in a phylogenetic context. *Syst Biol* 62:591–610
- Maddison WP (1991) Squared-change parsimony reconstructions of ancestral states for continuous-valued characters on a phylogenetic tree. *Syst Biol* 40:304–314
- Mattioli S (2011) Family Cervidae, deer. In: Wilson DE, Mittermeier RA (eds) *Handbook of the Mammals of the World – Volume 2. Hoofed Mammals*. Lynx Edicions, Barcelona, pp 350–443
- Mendoza M, Palmqvist P (2008) Hypsodonty in ungulates: an adaptation for grass consumption or for foraging in open habitat? *J Zool* 274:134–142
- Merino ML, Rossi RV (2010) Origin, systematics and morphological radiation. In: Duarte JMB, González S (eds) *Neotropical Cervidology. Biology and Medicine of Latin American Deer*. FUNEP & IUCN, Jaboticabal, pp 2–11
- Merino ML, Milne N, Vizcaíno SF (2005) A cranial morphometric study of deer (Mammalia, Cervidae) from Argentina using three-dimensional landmarks. *Acta Theriol* 50:91–108
- Olsen AM (2017) Feeding ecology is the primary driver of beak shape diversification in waterfowl. *Funct Ecol* 31:1985–1995
- R Core Team (2018) R: A Language and Environment for Statistical Computing. R Foundation for Statistical Computing, Vienna
- Radinsky LB (1969) The early evolution of the Perissodactyla. *Evolution* 23:308–328
- Radinsky LB (1985) Patterns in the evolution of ungulate jaw shape. *Am Zool* 25:303–314
- Radinsky LB (1987) *The Evolution of Vertebrate Design*. University of Chicago Press, Chicago
- Reddy DP, Kim J, Raaum R (2007) Resample.exe: <http://pages.nycep.org/nmg/programs.html>
- Rohlf FJ (1990) Rotational fit (Procrustes) methods. In: Rohlf FJ, Bookstein FL (eds) *Proceedings of the Michigan Morphometrics Workshop*. Univ Michigan Mus Zool Spec Publ 2: 227–236
- Schlager S (2017) Morpho and Rvcg - shape analysis in R. In: Zheng G, Li S, Székely G (eds) *Statistical Shape and Deformation Analysis*. Academic Press, London, pp 217–256
- Spencer LM (1995) Morphological correlates of dietary resource partitioning in the African Bovidae. *J Mammal* 76:448–471
- Vizcaíno SF, Bargo MS (2019) Views on the form-function correlation and biological design. *J Mammal Evol* <https://doi.org/10.1007/s10914-019-09487-4>
- Vizcaíno SF, Bargo MS, Cassini GH, Toledo N (2016) Forma y Función en Paleobiología de Vertebrados. Editorial de la Universidad Nacional de La Plata (EDULP), La Plata
- Warton DI, Hui FKC (2011) The arcsine is asinine: the analysis of proportions in ecology. *Ecology* 92:3–10
- Zurano JP, Magalhães FM, Asato AE, Silva G, Bidau CJ, Mesquita DO, Costa GC (2019) Cetartiodactyla: updating a time-calibrated molecular phylogeny. *Mol Phylogenet Evol* 133:256–262